AMERICAN SOCIETY FOR MICROBIOLOGY | Infection and Immunity

Bacteriology | Full-Length Text

IL-9 promotes methicillin-resistant *Staphylococcus aureus* pneumonia by regulating the polarization and phagocytosis of macrophages

Weihua Xu,[1] Keyin Tian,[1] Shaowen Hu,[2] Mingxiao Chen,[1] Meng Zhang[1]

AUTHOR AFFILIATIONS See affiliation list on p. 10.

ABSTRACT In this study, we examined the effect of *Il9* deletion on macrophages in methicillin-resistant *Staphylococcus aureus* (MRSA) infection. MRSA-infected mice were employed for the *in vivo* experiments, and RAW264.7 cells were stimulated with MRSA for the *in vitro* experiments. Macrophage polarization was determined by flow cytometry and quantitative real-time PCR; macrophage phagocytosis was assessed by flow cytometry and laser scanning confocal microscopy; cell apoptosis was assessed by flow cytometry and western blotting. *Il9* deletion markedly elevated macrophage phagocytosis and M2 macrophages in MRSA infection, which was accompanied by elevated expression of *Il10* and *Arg1* and reduced expression of *Inos*, tumor necrosis factor-α (*Tnfa)*, and *Il6*. *Il9* deletion also inhibited macrophage apoptosis in MRSA infection, which was manifested by elevated B-cell lymphoma 2 (BCL-2) protein level and reduced protein levels of cleaved cysteine protease 3 (CASPASE-3) and BCL2-Associated X (BAX). Both the *in vivo* and *in vitro* experiments further showed the activation of phosphoinositide 3-kinase (PI3K)/AKT (also known as protein kinase B, PKB) signaling pathway in MRSA infection and that the regulation of *Il9* expression may be dependent on Toll-like receptor (TLR) 2/PI3K pathway. The above results showed that *Il9* deletion exhibited a protective role against MRSA infection by promoting M2 polarization and phagocytosis of macrophages and the regulation of *Il9* partly owing to the activation of TLR2/PI3K pathway, proposing a novel therapeutic strategy for MRSA-infected pneumonia.

KEYWORDS *Il9*, MRSA, polarization, phagocytosis, macrophages, TLR2/PI3K pathway

Pneumonia is one of the main causes of death in children under 5 years old worldwide (1). *Staphylococcus aureus* has long been recognized as an important pathogen of pneumonia. However, with the extensive use of antibiotics, methicillin-resistant *Staphylococcus aureus* (MRSA) is prevalent and has been a major threat in recent decades (2). Most people have *Staphylococcus aureus* colonies, but only a few exhibit clinical diseases. Thus, enhancing the immune response is the key to solving MRSA infection rather than antibiotic treatment.

Mammalian immunity against extracellular bacterial infection can be divided into innate immunity and adaptive immunity (3, 4). Macrophages play an important role in innate immunity (5). Phagocytosis is an ancient and highly conserved process by which macrophages respond to bacterial infection through innate immune responses, and this process is accompanied by the secretion of proinflammatory and inflammatory cytokines, which is also an important feature of host resistance against pathogenic microorganisms (6, 7). In addition to innate immunity, adaptive immunity is recruited later to mediate long-term immune memory responses. Macrophages not only play an important role in the phagocytosis of bacteria but also act as antigen-presenting cells to activate T and B cells into effector cells (8). Generally, microbial pathogens are

Editor Kimberly A. Kline, Universite de Geneve, Geneva, Switzerland

Address correspondence to Weihua Xu, xwhua978@163.com.

The authors declare no conflict of interest.

See the funding table on p. 10.

Received 28 April 2023
Accepted 21 July 2023
Published 28 September 2023

intended to destroy the host defense system; therefore, a clear understanding of the interaction between MRSA and macrophages will provide a novel idea for the prevention and treatment of MRSA. However, there is a lack of previous studies on the regulatory mechanism of macrophages in MRSA infection.

Our previous study found that interleukin (IL)-9 was highly expressed in the serum, bronchoalveolar lavage fluid, and lung tissue of MRSA-infected mice, and pretreatment with an IL-9 neutralizing antibody largely reduced the number of macrophages and proinflammatory cytokines after MRSA infection (9), suggesting the participation of macrophages in MRSA infection. However, the effect of IL-9 on macrophage phagocytosis and polarization of *S. aureus* is still unclear. IL-9 is involved in the regulatory network of the phosphoinositide 3-kinase (PI3K)/AKT (also known as protein kinase B, PKB)/mammalian target of rapamycin (mTOR) signaling pathway (10). Toll-like receptor (TLR) 2 signaling, the main signaling pathway for the recognition of gram-positive bacteria, was confirmed to be associated with the activation of the PI3K/AKT pathway (11). Thus, we speculated that the TLR2-PI3K/AKT-IL-9 axis was involved in MRSA infection by regulating the polarization and phagocytosis of macrophages.

MATERIALS AND METHODS

Animals

Male BALB/c mice (6–10 weeks) were obtained from the Laboratory Animal Center of Anhui Medical University.

The establishment of pneumonia mouse model

The mouse model of pneumonia was established as previously described (9). A single colony of MRSA ST239 strain (ATCC, Manassas, USA) was grown to logarithmic phase in trypsin soy broth, and then the culture was resuspended in phosphate-buffered saline after the centrifugation. Finally, 5×10^8 colony-forming units (CFU) of ST239 strain were intranasally injected into the anesthetized BALB/c mice.

Experimental grouping

We divided BALB/c mice into four groupsvia different intravenous injection 24 h before MRSA infection: uninfected group (100 µL saline, $n = 6$), MRSA-infected group (100 µL saline, $n = 6$), IgG group (100 µL saline with 2 µg IgG, $n = 6$), and anti-IL-9 group (100 µL saline with 2 µg goat anti-mouse IL-9 neutralizing antibody, $n = 6$). After the infection, the mental state, appearance changes, and deaths of all mice were observed and recorded for 8 days.

Cell transfection

Short interfering RNAs (siRNAs) targeting *Il9* (*Il9* siRNA) and *Tlr2* (*Tlr2* siRNA) and their corresponding controls were purchased from GenePharma (Shanghai, China). For cell transfection, when the confluence of RAW264.7 cells reached 70%, *Il9* siRNA or *Tlr2* siRNA was transfected using Lipofectamine 3000 according to the manufacturer's protocols (Invitrogen, Carlsbad, CA).

Bacterial counting

Briefly, the homogenized lung tissues were plated evenly on the surface of tryptic soy broth plates at 37°C for 24 h, and then the colonies were counted.

Hematoxylin-eosin (H&E) staining

For H&E staining, 4-µm-thick sections were cut from paraffin-embedded lung tissues, and the sections were processed using an H&E staining kit (Sigma-Aldrich, St Louis, USA) and

scored by two blinded pathologists. The degree of lung injury was evaluated by the sum of severity score and range score as follows: severity score: 0 (no), 1 (mild), 2 (moderate), 3 (severe), 4 (extremely severe); range score: 0 (no), 1 (small range), 2 (large range).

Enzyme-linked immunosorbent assay (ELISA)

The lung tissues were homogenized and centrifuged at 4000 × *g* for 15 min at 4°C. The levels of transforming growth factor-beta (TGF-β), interferon-gamma (IFN-γ), IL-4, and IL-17 in the supernatant were measured using ELISA kits according to the manufacturer's instructions.

M1/M2 macrophage detection by flow cytometry

The proportions of M1 macrophages and M2 macrophages were measured by flow cytometry. Briefly, forward scatter (FSC) and side scatter (SSC) gates were used to remove cell debris and clumped cells to circle the target cell population. Then, FSC-A and FSC-H gates were used to circle the single-cell population. The cross gates of CD86 and F4/80 were used to circle M1 macrophages, namely $F4/80^{+}CD86^{+}$ cells, and the cross gates of CD206 and F4/80 were used to circle M2 macrophages, namely $F4/80^{+}CD206^{+}$ cells.

Phagocytosis experiments

Flow cytometry was performed to assess the phagocytic ability of macrophages. Firstly, FSC and SSC gates were used to remove cell debris and clumped cells to circle the target cell population. FSC-A and FSC-H gates were used to circle the single-cell population, and the cross gates of CD11b and F4/80 were used to circle macrophages. Then, according to the ratio of cell:bacteria (1:20), prestained *Staphylococcus aureus* with fluorescein 5-isothiocyanate (FITC) was added to macrophages for 30 min, and then 5 mM EDTA was added to stop the experiments. The cross gates of FITC and F4/80 were used to circle the FITC- and F4/80-positive cells, namely, $FITC^{+}F4/80^{+}$ cells. Additionally, laser scanning confocal microscopy was also employed to determine FITC- and F4/80-positive cells. However, neither flow cytometry nor laser scanning confocal microscopy differentiated surface-bound and internalized bacteria.

RNA isolation and quantitative real-time PCR (qRT-PCR)

We extracted total RNA from lung tissues and RAW264.7 cells using TRIzol reagent (Invitrogen), and then employed a PrimeScript RT reagent kit (Takara) to obtain cDNA. The mRNA expression levels of *Il9, Il10, Il6, Inos, Arg1, Tnfa*, and *Tlr2* were measured using an Applied Biosystems 7500 Real Time PCR System (Applied Biosystems) with SYBR Green QPCR Master Mix (Invitrogen). The mRNA expression of gene was normalized to *Gapdh* using the $2^{-\Delta\Delta Ct}$ method.

Il9 (forward): 5′-ACGGTGTGGTACAATCATC-3′
Il9 (reverse): 5′-TTGGTGACATACATCCTTG-3′
Tnfa (forward): 5′-AAGCCTGTAGCCCACGTCGTA-3′
Tnfa (reverse): 5′-AGGTACAACCCATCGGCTGG-3′
Il10 (forward): 5′-ATGCTGCCTGCTCTTACTGACTG-3′
Il10 (reverse): 5′-CCCAAGTAACCCTTAAAGTCCTGC-3′
Arg1 (forward): 5′-TGTCCCTAATGACAGCTCCTT-3′
Arg1 (reverse): 5′-GCATCCACCCAAATGACACAT-3′
Il6 (forward): 5′-CTGCAAGAGACTTCCATCCAG-3′
Il6 (reverse): 5′-AGTGGTATAGACAGGTCTGTTGG-3′
Inos (forward): 5′-CTCAGCCCAACAATACAAG-3′
Inos (reverse): 5′-CTACAGTTCCGAGCGTCA-3′
Tlr2 (forward): 5′-AGGTGCGGACTGTTTCCTTC-3′
Tlr2 (reverse): 5′-AGATTTGACGCTTTGTCTGAGG-3′
Gapdh (forward): 5′-TCGTCCCGTAGACAAAATGG-3′

Gapdh (reverse): 5´-TTGAGGTCAATGAAGGGGTC-3´

Western blot

The total proteins from tissues or cells were extracted by radio immunoprecipitation assay (RIPA) lysis buffer (Beyotime, China), and the quality of the protein was measured by bicinchoninic acid disodium (BCA) (Sigma-Aldrich). Equal amounts of proteins were resolved by SDS-PAGE, transferred onto a nitrocellulose membrane and incubated with primary antibodies specific for cleaved cysteine protease 3 (CASPASE-3) (ab214430, 1:5,000; Abcam, USA), BCL2-Associated X (BAX) (ab32503, 1:1,000; Abcam, USA), B-cell lymphoma 2 (BCL-2) (ab182858, 1:2,000; Abcam, USA), PI3K (ab191606, 1:1,000; Abcam, USA), p-PI3K (ab182651, 1:1,000; Abcam, USA), AKT (sc-5298, 1:500; Santa Cruz Biotechnology, CA), p-AKT (sc-514032, 1:500; Santa Cruz Biotechnology, CA), mTOR (sc-517464, 1:1,000; Santa Cruz Biotechnology, CA), and GAPDH (sc-47724, 1:1,000, Santa Cruz Biotechnology). The secondary antibody was horseradish peroxidase (HRP)-conjugated goat anti-rabbit IgG (ab150077). The proteins were quantified using Quantity One software (Bio-Rad Laboratories). GAPDH was the internal control.

Statistical analysis

We analyzed the differences between groups using unpaired Student's *t*-tests or one-way analysis of variance using SPSS software version 19.0 (IBM, Chicago, USA). All results were expressed as the mean ± standard deviation (SD). Significant *P*-value was less than 0.05.

RESULTS

Anti-IL-9 antibody reduced lung inflammation in MRSA-infected mice

Mice in the control group were normal and did not have any symptoms after inoculation. However, most of the MRSA-infected mice exhibited poor mental state and less diet

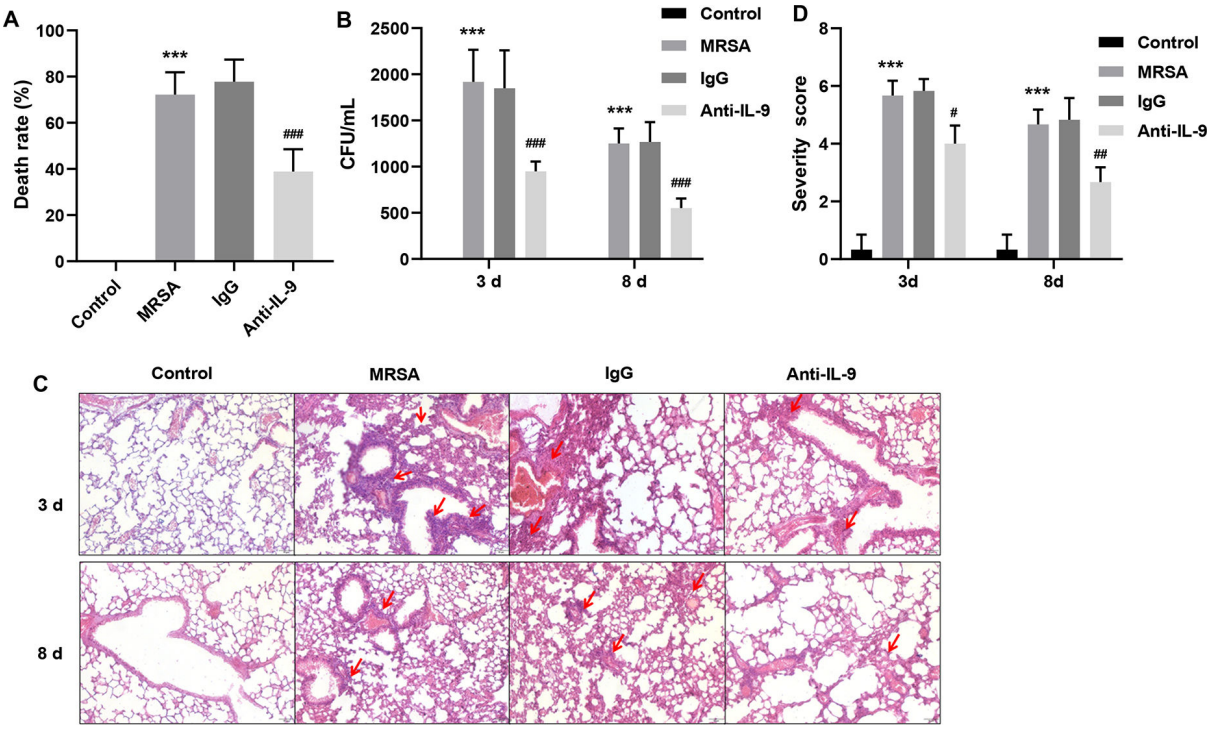

FIG 1 Anti-IL-9 antibody reduced lung inflammation in MRSA-infected mice. The death rate (A) and the amount of bacteria (B) in the lung tissues of mice in different groups (n = 6 per group) were calculated. The lung pathological changes were assessed by hematoxylin and eosin staining (C) and pathological score (D) in different groups, the red arrows indicated the inflammatory infiltration. Scale bar = 50 µm. Data were represented as the mean ± SD. ***$P < 0.001$ vs the MRSA group; #$P < 0.05$, ##$P < 0.01$, ###$P < 0.001$ vs the IgG group.

after the inoculation for 2 days, and the number of deaths peaked on day 6, but the remaining mice stopped dying after 8 days. To our surprise, the IL-9 neutralizing antibody significantly reduced the death of MRSA-infected mice, which is illustrated in Fig. 1A. In addition, the IL-9 neutralizing antibody markedly decreased the number of CFUs in the lung tissues of MRSA-infected mice after inoculation for 3 and 8 days (Fig. 1B). H&E staining further revealed the obvious improvement of inflammatory cell infiltration in the lung tissues of MRSA-infected mice by IL-9 neutralizing antibody (Fig. 1C), which was further confirmed by the pathological score (Fig. 1D), both on day 3 and day 8 after inoculation. The above data suggested that IL-9 neutralizing antibody improved lung inflammation in MRSA-infected mice.

Anti-IL-9 antibody promoted macrophage M1 to M2 polarization in MRSA-infected mice

Then, we investigated the effect of IL-9 neutralizing antibody on macrophage polarization in MRSA-infected mice. The results showed that, compared with the IgG group, the IL-9 neutralizing antibody group showed markedly increased CD206-positive cells (Fig. 2A and B) but decreased CD86-positive cells (Fig. 2C and D) in the lung tissues of MRSA-infected mice. In addition, compared with the IgG group, *Il10* (Fig. 2E) and *Arg1* (Fig. 2F) mRNA expression levels were significantly elevated, while *Inos* (Fig. 2G), *Tnfa* (Fig. 2H), and *Il6* (Fig. 2I) mRNA expression was obviously downregulated in the anti-IL-9 group. The above data suggested that neutralization of IL-9 significantly promoted macrophage M1 to M2 polarization in the lung tissues of MRSA-infected mice.

Anti-IL-9 antibody promoted phagocytosis and inhibited apoptosis of macrophages in MRSA-infected mice

Next, we further explored the effect of the IL-9 neutralizing antibody on macrophage phagocytosis in MRSA-infected mice. Alveolar macrophages isolated from mice were cocultured with MRSA, and both flow cytometry and laser scanning confocal microscopy were performed to assess macrophage phagocytosis. The results showed that, compared

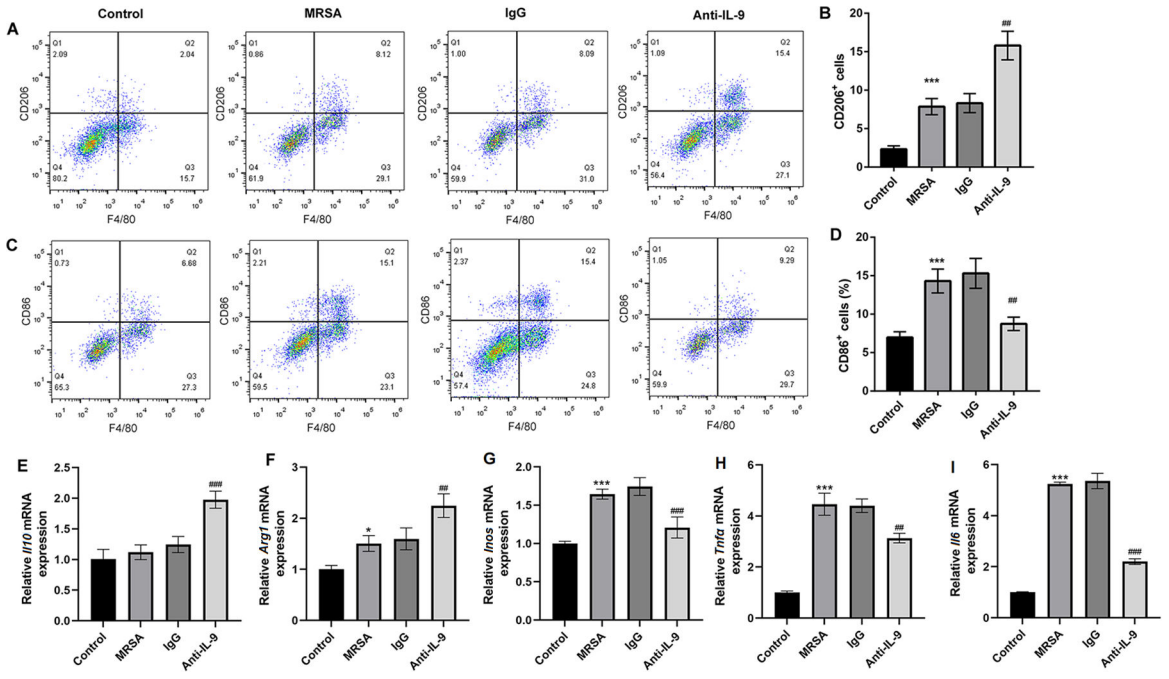

FIG 2 Anti-IL-9 antibody promoted M2 macrophage polarization in MRSA-infected mice. The number of CD86- and CD206-positive cells in the lung tissues of mice (n = 6 per group) were determined by flow cytometry (A–D), respectively. The mRNA expression levels of *Il10* (E), *Arg1* (F), *Inos* (G), *Tnfa* (H), and *Il6* (I) in the lung tissues of mice were determined by qRT-PCR. Data are represented as the mean ± SD. *$P < 0.05$, ***$P < 0.001$ vs the MRSA group; ##$P < 0.01$ vs the IgG group.

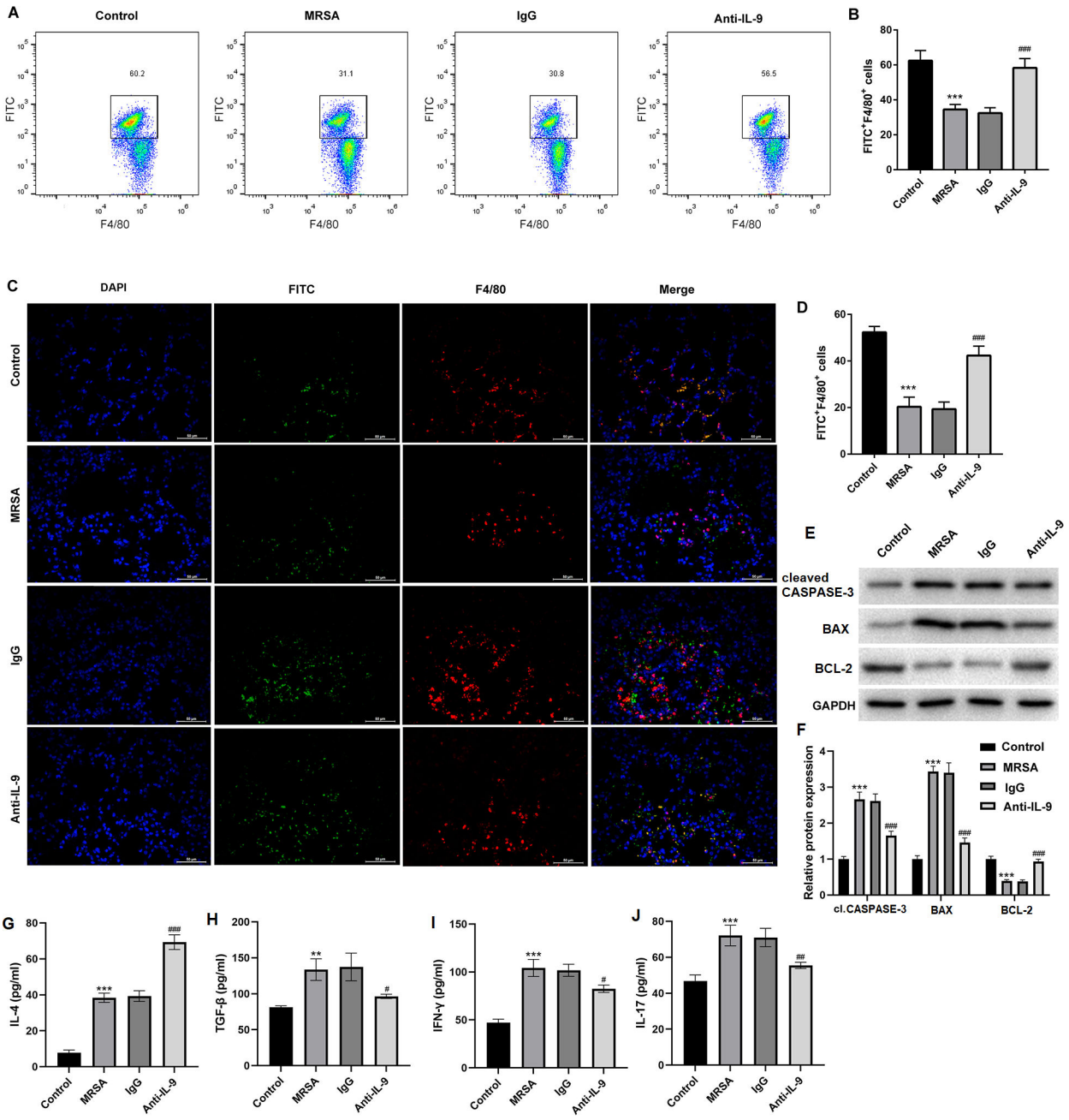

FIG 3 Anti-IL-9 antibody promoted phagocytosis and inhibited apoptosis of macrophages in MRSA-infected mice. Alveolar macrophages isolated from mice (n = 6 per group) were cocultured with MRSA prestained with FITC, and macrophage phagocytosis was assessed by flow cytometry (A and B) and laser scanning confocal microscopy (C and D), but they did not differentiate surface-bound and internalized bacteria. The protein levels of cleaved CASPASE-3, BAX, and BCL-2 and the expression of IL-4, TGF-β, IFN-γ, and IL-17 in the lung tissues of mice were detected by western blot (E and F) and ELISA (G–J), respectively. Data are represented as the mean ± SD. $^{**}P < 0.01$, $^{***}P < 0.001$ vs the MRSA group; $\#P < 0.05$, $\#\#P < 0.01$, $\#\#\#P < 0.001$ vs the IgG group.

with the IgG group, the IL-9 neutralizing antibody group showed markedly enhanced macrophage phagocytosis (Fig. 3A through D). Furthermore, compared with the IgG group, the protein levels of cleaved CASPASE-3 and BAX were significantly downregulated, while the BCL-2 protein level was elevated in the anti-IL-9 group, suggesting the inhibitory effect of the IL-9 neutralizing antibody on macrophage apoptosis in MRSA-infected mice (Fig. 3E and F). Additionally, significant elevation of IL-4 (Fig. 3G) and

reduction of TGF-β (Fig. 3H), IFN-γ (Fig. 3I), and IL-17 (Fig. 3J) were observed in the lung tissues of MRSA-infected mice treated with the IL-9 neutralizing antibody.

Il9 deletion promoted macrophage M1 to M2 polarization in MRSA-infected RAW264.7 cells

To further determine the promoting effect of *Il9* loss on M2 macrophages in MRSA-induced pneumonia, RAW264.7 cells infected with MRSA were adopted for *in vitro* experiments, and *Il9* siRNA was employed to delete *Il9*. As expected, si-*Il9* significantly reduced *Il9* mRNA expression levels in MRSA-infected RAW264.7 cells (Fig. 4A). Si-*Il9* also significantly increased CD206-positive cells (Fig. 4B and C) and decreased CD86-positive cells (Fig. 4D and E), which were further confirmed by increased mRNA expression levels of *Arg1* (Fig. 4F) and decreased mRNA expression levels of *Inos* (Fig. 4G) in MRSA-infected RAW264.7 cells. Furthermore, compared with the siRNA negative control (Si-NC) group, significantly elevated mRNA expression levels of *Il10* and downregulated mRNA expression levels of *Tnfa* and *Il6* were also observed in the Si-*Il9* group (Fig. 4H). These data suggested that *Il9* knockdown elevated M2 macrophages in MRSA-infected RAW264.7 cells.

Il9 deletion promoted phagocytosis and inhibited apoptosis of macrophages in MRSA-infected RAW264.7 cells

Similar to the *in vivo* experiments, the flow cytometry results of the *in vitro* experiments revealed that, compared with Si-NC, Si-*Il9* markedly enhanced the phagocytosis of MRSA-infected RAW264.7 cells (Fig. 5A and B). Flow cytometry results also revealed that si-*Il9* markedly inhibited the apoptosis of MRSA-infected RAW264.7 cells (Fig. 5C and D), which was further confirmed by the significantly elevated BCL-2 protein level and downregulated protein levels of cleaved CASPASE-3 and BAX in the si-*Il9* group (Fig. 5E and F).

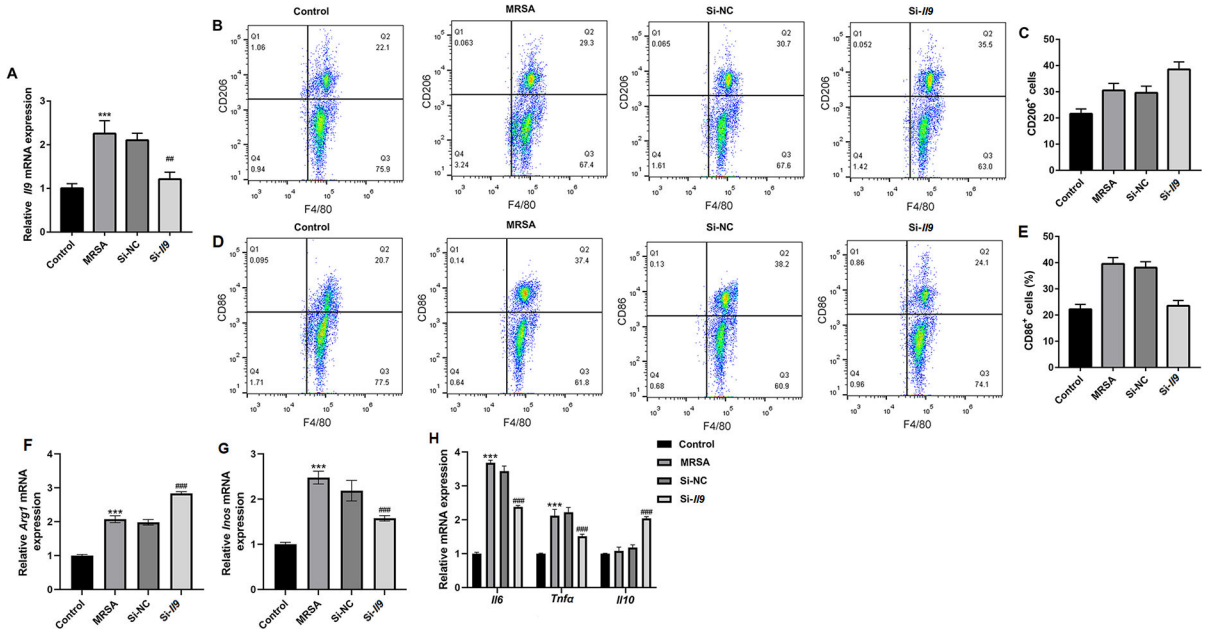

FIG 4 *Il9* deletion promoted M2 macrophage polarization in MRSA-infected RAW264.7 cells. RAW264.7 cells were infected with MRSA, and *Il9* siRNA was employed to delete *Il9* in RAW264.7 cells. qRT-PCR was performed to examine the mRNA expression levels of *Il9* (A), *Arg1* (F), *Inos* (G), *Il10*, *Tnfa,* and *Il6* (H); flow cytometry was performed to detect the number of F4/80$^+$CD206$^+$ (B and C) cells and F4/80$^+$CD86$^+$ cells (D and E). Data are represented as the mean ± SD. $n = 3$. ***$P < 0.001$ vs the MRSA group; ###$P < 0.001$ vs the Si-NC group.

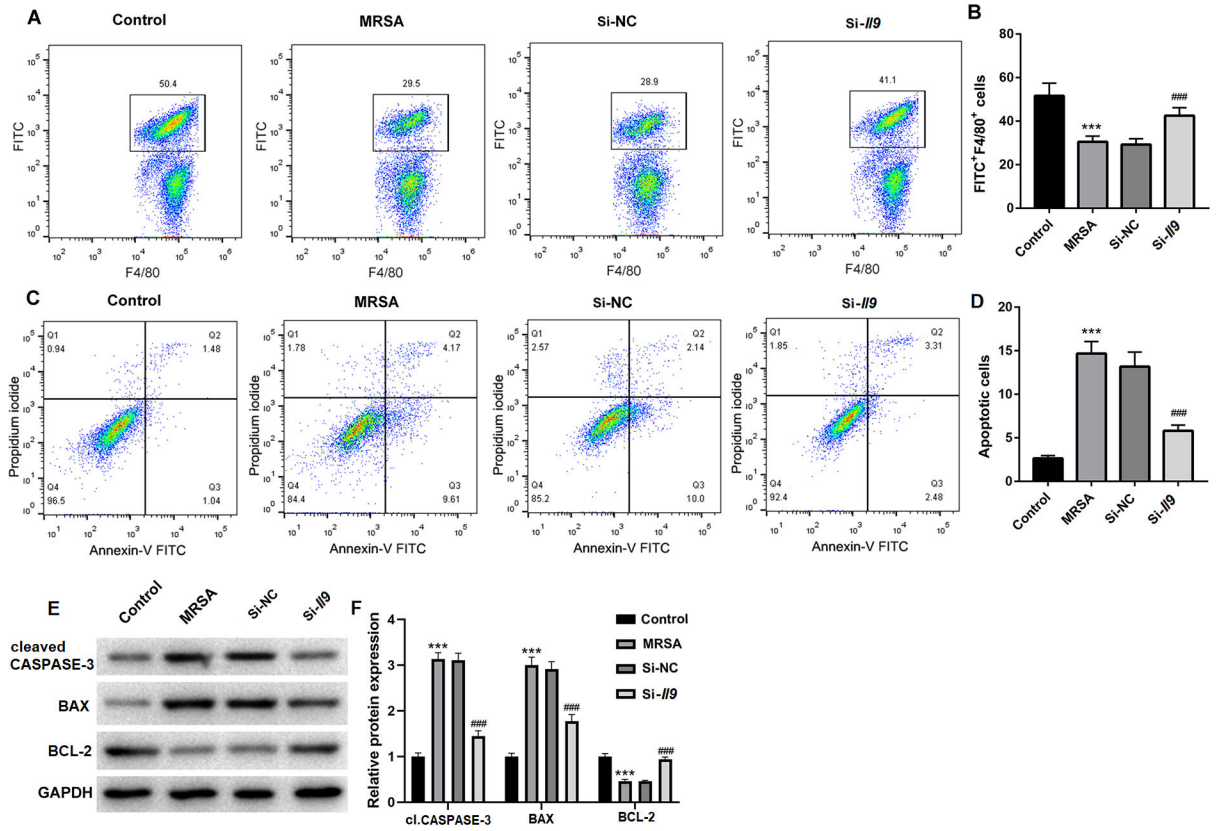

FIG 5 *Il9* deletion promoted phagocytosis and inhibited apoptosis in MRSA-infected RAW264.7 cells. RAW264.7 cells were infected with MRSA, and *Il9* siRNA was employed to delete *Il9* in RAW264.7 cells. Flow cytometry was performed to assess the phagocytosis ability (A and B) and apoptosis (C and D) of RAW264.7 cells. (E and F) The protein levels of cleaved CASPASE-3, BAX, and BCL-2 in RAW264.7 cells were detected by western blot. Data are represented as the mean ± SD. $n = 3$. ***$P < 0.001$ vs the MRSA group; ### $P < 0.001$ vs the Si-NC group.

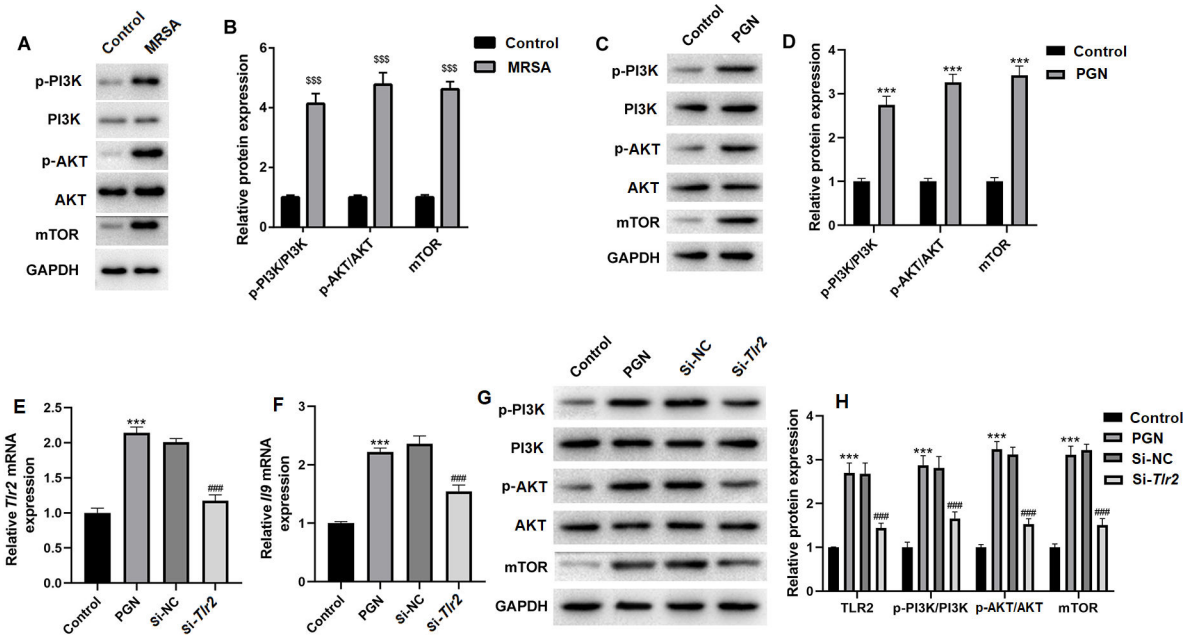

FIG 6 The regulation of *Il9* was dependent on the TLR2/PI3K pathway. The protein levels of p-PI3K, p-AKT, and mTOR in the lung tissues of mice (A and B) and RAW264.7 cells (C and D) were detected by western blot. Si-*Tlr2* was used to delete *Tlr2* in RAW264.7 cells, and the mRNA expression levels of *Tlr2* (E) and *Il9* (F) was measured by qRT-PCR. (G and H) The protein levels of TLR2, p-PI3K, p-AKT, and mTOR in RAW264.7 cells were detected by western blot. Data are represented as the mean ± SD. $n = 3$. ***$P < 0.001$ vs the control group; ### $P < 0.001$ vs the si-NC group.

The regulation of *Il9* was dependent on the TLR2/PI3K pathway

Additionally, we also observed elevated protein levels of p-PI3K, p-AKT, and mTOR in the lung tissues of MRSA-infected mice (Fig. 6A and B), suggesting activation of the PI3K/AKT signaling pathway in MRSA infection. Furthermore, similar results were observed in RAW264.7 cells treated with peptidoglycan (PGN), which is derived from the *Staphylococcus aureus* cell wall (Fig. 6C and D). Considering that TLR2 acted as the main signaling pathway for the recognition of gram-positive bacteria, we speculate that TLR2 may affect the PI3K/AKT signaling pathway in MRSA infection. Si-*Tlr2* was used to delete *Tlr2* in RAW264.7 cells treated with PGN (Fig. 6E). Furthermore, we found that Si-*Tlr2* not only eliminated PGN-induced expression of *Il9* (Fig. 6F) but also reversed the elevated protein levels of p-PI3K, p-AKT, and mTOR induced by PGN (Fig. 6G and H).

DISCUSSION

Staphylococcus aureus is the most common pathogenic bacterium in clinical practice. It stimulates the human immune system to cause organ and tissue infections, including skin infections (12), lung infections (13), endocarditis (14), osteomyelitis (15), and other diseases, triggering a systemic inflammatory response and eventually leading to multiple organ failure and death. Furthermore, MRSA has severe resistance to β-lactams, aminoglycosides, macrolides, and other antibiotics; thus, it is called "super bacteria," and it makes clinical treatment very difficult (16). However, the mechanism of drug resistance and effective treatment of MRSA have not been elucidated.

Considering the severe drug resistance of MRSA, perhaps, enhancing own immunity is the key to solving MRSA infection apart from antibiotic treatment. Macrophages play an important role in the immune system against extracellular bacteria, including innate immunity and adaptive immunity. Our previous study found that IL-9 neutralizing antibodies largely reduced the number of macrophages and attenuated inflammation in MRSA-infected pneumonia (9), suggesting the participation of macrophages in MRSA-infected pneumonia. However, the specific molecular mechanisms related to macrophages by which IL-9 neutralizing antibodies attenuate pneumonia in MRSA-infected patients are still unclear. In addition to serving as phagocytes to defend against bacterial infection, macrophage polarization has also been observed in bacteria-infected diseases (17–19). Activated macrophages can generally be divided into two groups: classically activated macrophages (M1) and alternatively activated macrophages (M2). M1 macrophages are characterized by increased expression of nitric oxide, reactive oxygen species, and proinflammatory cytokines, such as TNF-α, interleukin-1 (IL-1), and interleukin-6 (IL-6)(20, 21), while M2 macrophages exhibit immunosuppressive activity and increased expression of IL-4, IL-10, and Arg-1 (22, 23). For instance, M2 macrophages were beneficial for controlling MRSA infection in mice with severe burn injury (24); exosomal miR-21 secreted by IL-1β-stimulated mesenchymal stem cells resulted in M2 polarization and ameliorated sepsis (25); and exosomal miR-30d-5p contributed to sepsis-related acute lung injury (ALI) by inducing M1 macrophage polarization and priming macrophage pyroptosis through activating nuclear factor-kappaB (NF-κB) signaling. The above findings suggest the beneficial role of M2 macrophages in infection-related diseases. As expected, in this study, the IL-9 neutralizing antibody not only elevated phagocytosis but also induced M2 polarization of macrophages in lung tissues of MRSA-infected mice, which were also accompanied by elevated *Il10* and *Arg1* and downregulated *Inos*, *Tnfa*, and *Il6*, in comparison with MRSA-infected mice treated with IgG. Additionally, our results also revealed the significant elevation of IL-4 and reduction of TGF-β, IFN-γ, and IL-17 in lung tissues of MRSA-infected mice treated with the IL-9 neutralizing antibody, indicating that IL-9-regulated macrophages may be a direct regulator of the inflammatory response during MRSA infection. The *in vitro* experiments further confirmed the promoting effect of *Il9* deletion on phagocytosis and M2 polarization of macrophages in MRSA infection.

The surface of macrophages contains a large number of pattern recognition receptors, including Dectin-1, scavenger-like receptors, TLRs, and nucleotide-binding and oligomerization domain (NOD)-like family receptors, and TLRs can specifically recognize lipopolysaccharides, flagellins, and hypomethylated DNA glycoskeletons, among which TLR2 is one of the important immune receptors on the surface of macrophages and activates innate immune responses by recognizing and binding pathogen-associated molecular patterns (26, 27). TLR2 can protect against pathogenic microorganisms by regulating autophagy and phagocytosis by macrophages (28, 29). It has been reported that TLR2 recruits the transduction molecule myeloid differentiation factor 88 and subsequently activates the downstream signaling protein PI3K to promote phagocytosis of murine macrophages (30). PI3K is one of the key enzymes involved in various intracellular signal transduction and transformation pathways and plays an important biological role in cell growth, survival, proliferation, apoptosis, and metabolism (31). PI3K also plays an important role in the immune response and participates in the regulation of inflammatory factors, thereby contributing to the elimination of invading pathogenic microorganisms (32). However, whether TLR2, on the surface of macrophages, regulates MRSA-infected inflammation through the downstream PI3K signaling pathway remains unclear. Thus, we stimulated RAW264.7 cells with PGN and found that *Il9* expression and the protein levels of TLR2, p-PI3K, p-AKT, and mTOR were all markedly elevated. We also found that si-*Tlr2* not only reversed the elevated protein levels of p-PI3K, p-AKT, and mTOR induced by PGN but also eliminated PGN-induced expression of *Il9*. These results reveal that the regulation of *Il9* may be dependent on the TLR2/PI3K pathway in macrophages.

In conclusion, in the present study, our results demonstrate that *Il9* deletion significantly promotes phagocytosis and M2 polarization of macrophages in MRSA infection, which may be dependent on the TLR2/PI3K pathway. However, there are several limitations in this study. First, more studies on the correlation between the TLR2/PI3K pathway and *Il9* are required to make our conclusion more reliable. Moreover, the specific mechanism by which the TLR2/PI3K pathway regulates the phagocytosis and polarization of macrophages needs to be further explored.

ACKNOWLEDGMENTS

This study was supported by the grant from the Key Research and Development Program Projects in Anhui Province (No.1804h08020285).

AUTHOR AFFILIATIONS

[1]Department of Emergency, Anhui Provincial Children's Hospital, Hefei, Anhui, China
[2]Department of Neonatology, Anhui Provincial Children's Hospital, Hefei, Anhui, China

AUTHOR ORCIDs

Weihua Xu http://orcid.org/0000-0001-8490-0097

FUNDING

Funder	Grant(s)	Author(s)
Key Research and Development Program Projects in Anhui Province	1804h08020285	Weihua Xu

DATA AVAILABILITY

The data used to support the findings of this study are available from the corresponding author upon reasonable request.

ETHICS APPROVAL

All experimental protocols were approved by the Ethics Committee of Anhui Children's Hospital.

REFERENCES

1. Dahman HAB. 2017. Challenges in the diagnosis and management of pediatric rheumatology in the developing world: lessons from a newly established clinic in Yemen. Sudan J Paediatr 17:21–29. https://doi.org/10.24911/SJP.2017.2.2
2. Vestergaard M, Frees D, Ingmer H. 2019. Antibiotic resistance and the MRSA problem. Microbiol Spectr 7. https://doi.org/10.1128/microbiolspec.GPP3-0057-2018
3. Wang L, Wang K, Zou Z-Q. 2015. Crosstalk between innate and adaptive immunity in hepatitis B virus infection. World J Hepatol 7:2980–2991. https://doi.org/10.4254/wjh.v7.i30.2980
4. Schmaler M. 2010. International conference on science & social research. https://doi.org/10.1371/journal.pone.0015159
5. Zumerle S, Calì B, Munari F, Angioni R, Di Virgilio F, Molon B, Viola A. 2019. Intercellular calcium signaling induced by ATP potentiates macrophage phagocytosis. Cell Rep 27:1–10. https://doi.org/10.1016/j.celrep.2019.03.011
6. Yang H-C, Park CH, Hongxuan Q, Yongjoon K. 2018. Immunomodulation of Biomaterials by controlling macrophage polarization. Adv Exp Med Biol. https://doi.org/10.1007/978-981-13-0445-3_12
7. Xie H, Zhang J, Xie X, Jin S, Anesthesiology DO. 2016. Maresin 1 strengthen macrophages phagocytosis via miR-340. Journal of Wenzhou Medical University.
8. Li J, Chen J, Yang G, Tao L. 2021. Sublancin protects against methicillin-resistant *Staphylococcus aureus* infection by the combined modulation of innate immune response and microbiota. Peptides 141:170533. https://doi.org/10.1016/j.peptides.2021.170533
9. Xu W, Tian K, Li X, Zhang S. 2020. IL-9 blockade attenuates inflammation in a murine model of methicillin-resistant *Staphylococcus aureus* pneumonia. Acta Biochim Biophys Sin (Shanghai) 52:133–140. https://doi.org/10.1093/abbs/gmz149
10. Bi E, Ma X, Lu Y, Yang M, Wang Q, Xue G, Qian J, Wang S, Yi Q. 2017. Foxo1 and Foxp1 play opposing roles in regulating the differentiation and antitumor activity of TH9 cells programmed by IL-7. Sci Signal 10:eaak9741. https://doi.org/10.1126/scisignal.aak9741
11. Zhai N, Li H, Song H, Yang Y, Cui A, Li T, Niu J, Crispe IN, Su L, Tu Z. 2017. Hepatitis C virus induces MDSCs-like monocytes through TLR2/PI3K/AKT/STAT3 signaling. PLoS One 12:e0170516. https://doi.org/10.1371/journal.pone.0170516
12. EugeneV-M, GregoryK-R, Emad M-E, Carey D-S, Jason W-B. 2017. Genomic characterization of Usa300 MRSA to evaluate Intraclass transmission and recurrence of SSTI among high risk military Trainees. Clin Infect Dis 65:461–468. https://doi.org/10.1093/cid/cix327
13. Zeng S, Chen D, Liu G, Wu Y-X, Gao Z-Q, Su Y, Yuan J-N, Liu L, Shan J-C, Pang Q-F, Zhu T. 2021. Salvinorin A protects against methicillin resistant *Staphylococcus aureus* -induced acute lung injury via Nrf2 pathway. Int Immunopharmacol 90:107221. https://doi.org/10.1016/j.intimp.2020.107221
14. Górgolas M, P A, Verdejo C, ., Guerrero M. 2021. Treatment of experimental endocarditis due to methicillin-susceptible or methicillin-resistant *Staphylococcus aureus* with trimethoprim-sulfamethoxazole and antibiotics that inhibit cell wall synthesis
15. Yan L, Jiang D-M, Cao Z-D, Wu J, Wang X, Wang Z-L, Li Y-J, Yi Y-F. 2015. Treatment of *Staphylococcus aureus*-induced chronic osteomyelitis with bone-like hydroxyapatite/poly amino acid loaded with rifapentine microspheres. Drug Des Devel Ther 9:3665–3676. https://doi.org/10.2147/DDDT.S84486
16. Sarkissian EJ, Gans I, Gunderson MA, Myers SH, Spiegel DA, Flynn JM. 2016. Community-acquired methicillin-resistant *Staphylococcus aureus* musculoskeletal infections: emerging trends over the past decade. J Pediatr Orthop 36:323–327. https://doi.org/10.1097/BPO.0000000000000439
17. Trivedi NH, Yu J-J, Hung C-Y, Doelger RP, Navara CS, Armitige LY, Seshu J, Sinai AP, Chambers JP, Guentzel MN, Arulanandam BP. 2018. Microbial co-infection alters macrophage polarization, phagosomal escape, and microbial killing. Innate Immun 24:152–162. https://doi.org/10.1177/1753425918760180
18. Murray PJ, Allen JE, Biswas SK, Fisher EA, Gilroy DW, Goerdt S, Gordon S, Hamilton JA, Ivashkiv LB, Lawrence T, Locati M, Mantovani A, Martinez FO, Mege J-L, Mosser DM, Natoli G, Saeij JP, Schultze JL, Shirey KA, Sica A, Suttles J, Udalova I, van Ginderachter JA, Vogel SN, Wynn TA. 2014. Macrophage activation and polarization: nomenclature and experimental guidelines. Immunity 41:14–20. https://doi.org/10.1016/j.immuni.2014.06.008
19. Atri C, Guerfali FZ, Laouini D. 2018. Role of human macrophage polarization in inflammation during infectious diseases. Int J Mol Sci 19:1801. https://doi.org/10.3390/ijms19061801
20. Yang S, Li J, Chen Y, Zhang S, Feng C, Hou Z, Cai J, Wang Y, Hui R, Lv B, Zhang W. 2019. Microrna-216a promotes M1 macrophages polarization and atherosclerosis progression by activating telomerase via the Smad3/NF-kB pathway. Biochim Biophys Acta Mol Basis Dis 1865:1772–1781. https://doi.org/10.1016/j.bbadis.2018.06.016
21. Ch A, Ys A, Jin WA, Xz A, Wl A, Cz A, Li GB, Yi YA. 2021. Nox4 promotes mucosal barrier injury in inflammatory bowel disease by mediating macrophages M1 polarization through ROS. ScienceDirect. https://doi.org/10.1016/j.intimp.2021.108361IF:5.6%20Q1 B2
22. Mukhuty A, Fouzder C, Kundu R. 2021. Fetuin-A secretion from B-cells leads to accumulation of macrophages in islets, aggravates inflammation and impairs insulin secretion. J Cell Sci 134:jcs258507. https://doi.org/10.1242/jcs.258507%20IF: 4.0 Q3 B2 IF: 4.0 Q3 B2
23. Oishi S, Takano R, Tamura S, Tani S, Iwaizumi M, Hamaya Y, Takagaki K, Nagata T, Seto S, Horii T, Osawa S, Furuta T, Miyajima H, Sugimoto K. 2016. M2 polarization of murine peritoneal Macrophages induces regulatory cytokine production and suppresses T-cell proliferation. Immunology 149:320–328. https://doi.org/10.1111/imm.12647
24. Nishiguchi T, Ito I, Lee JO, Suzuki S, Suzuki F, Kobayashi M. 2017. Macrophage polarization and MRSA infection in burned mice. Immunol Cell Biol 95:198–206. https://doi.org/10.1038/icb.2016.84
25. Yao M, Cui B, Zhang W, Ma W, Zhao G, Xing L. 2021. Exosomal miR-21 secreted by IL-1B-primed-mesenchymal stem cells induces macrophage M2 polarization and ameliorates sepsis. Life Sci 264:118658. https://doi.org/10.1016/j.lfs.2020.118658
26. Jones BW, Heldwein KA, Means TK, Saukkonen JJ, Fenton MJ. 2001. Differential roles of toll-like receptors in the elicitation of proinflammatory responses by macrophages. Ann Rheum Dis 60 Suppl 3:iii6–12. https://doi.org/10.1136/ard.60.90003.iii6
27. Shin D-M, Yang C-S, Yuk J-M, Lee J-Y, Kim KH, Shin SJ, Takahara K, Lee SJ, Jo E-K. 2008. Mycobacterium abscessus activates the macrophage innate immune response via a physical and functional interaction between TLR2 and dectin-1. Cell Microbiol 10:1608–1621. https://doi.org/10.1111/j.1462-5822.2008.01151.x
28. Fang L, Wu H-M, Ding P-S, Liu R-Y. 2014. TLR2 mediates phagocytosis and autophagy through JNK signaling pathway in *Staphylococcus aureus*-stimulated RAW264.7 cells. Cell Signal 26:806–814. https://doi.org/10.1016/j.cellsig.2013.12.016
29. Lu Z, Xie D, Chen Y, Tian E, Muhammad I, Chen X, Miao Y, Hu W, Wu Z, Ni H, Xin J, Li Y, Li J. 2017. TLR2 mediates autophagy through ERK signaling pathway in mycoplasma gallisepticum-infected RAW264.7 cells. Mol Immunol 87:161–170. https://doi.org/10.1016/j.molimm.2017.04.013
30. Shen Y, Kawamura I, Nomura T, Tsuchiya K, Hara H, Dewamitta SR, Sakai S, Qu H, Daim S, Yamamoto T, Mitsuyama M. 2010. Toll-like receptor 2-and MyD88-dependent phosphatidylinositol 3-kinase and Rac1 activation facilitates the phagocytosis of listeria monocytogenes by murine macrophages. Infect Immun 78:2857–2867. https://doi.org/10.1128/IAI.01138-09
31. Huang SH, Zhang T, Zhao CG, Qin J, Qi P, Li FT, He XJ. 2018. Aclidinium bromide inhibits human glioma cell proliferation, migration and

invasion and promotes apoptosis via the PI3K/AKT signaling pathway. Neoplasma 65:865–871. https://doi.org/10.4149/neo_2018_171117N705
32. Zhang X, Ming Y, Fu X, Niu Y, Lin Q, Liang H, Luo X, Liu L, Li N. 2022. PI3K/AKT/p53 pathway inhibits infectious spleen and kidney necrosis virus infection by regulating autophagy and immune responses. Fish Shellfish Immunol 120:648–657. https://doi.org/10.1016/j.fsi.2021.12.046